

# Relativistic Nucleus-Nucleus Collisions: Zone of Reactions and Space-Time Structure of a Fireball

D. Anchishkin<sup>1</sup>, A. Muskeyev<sup>2</sup>, and S. Yezhov<sup>2</sup>

<sup>1</sup>*Bogolyubov Institute for Theoretical Physics, Kiev 03680, Ukraine and*

<sup>2</sup>*Taras Shevchenko Kiev National University, Kiev 03022, Ukraine*

(Dated: March 3, 2022)

A zone of reactions is determined and then exploited as a tool in studying the space-time structure of an interacting system formed in a collision of relativistic nuclei. The time dependence of the reaction rates integrated over spatial coordinates is also considered. Evaluations are made with the help of the microscopic transport model UrQMD. The relation of the boundaries of different zones of reactions and the hypersurfaces of sharp chemical and kinetic freeze-outs is discussed.

PACS numbers: 25.75.-q, 25.75.Ag, 24.10.Lx

**Introduction.** In the collision of nuclei at high energies, a strongly excited system of interacting particles is formed. In fact, a fireball is identified with the zone of reactions by such a definition, i.e. with a space-time region, in which the reactions of particles occur. Hence, the zone of reactions must reflect the space-time characteristics of a fireball, and its study gives information about the evolution of the interacting system.

While studying the evolution of a fireball, it is important to know the size of the regions where the majority of the various processes are running. Depending on the model describing the system, we can distinguish the regions of the formation of a fireball, its isotropization and thermalization, the creation of particles, the regions of a chemical freeze-out and a kinetic one, etc. This allows us to conditionally select the stages of evolution of the system and, hence, to obtain the limits of validity of simple phenomenological models used for the description of the complicated physical phenomenon, as well as to describe separate stages of development of the system in more detail. In particular, the stages of formation ( $\tau \sim 0.1$  fm/c) and thermalization ( $\tau \sim 1$  fm/c) are most often described with the use of microscopic models based on the processes of interaction of quarks and gluons [1–3]. To describe the stage of spreading of a dense medium ( $1 \leq \tau \leq 7$  fm/c), the relativistic hydrodynamics is most often in use [4–6]. The further evolution of a hadron gas and the process of kinetic freeze-out ( $\tau \sim 20$ – $25$  fm/c) are covered by kinetic models [7, 8]. As parameters for the determination of the stages of evolution of a system, one can take the energy density, mean free path, rate of collisions of particles, etc.

In the present work, we use the hadron reaction rate (number of reactions in a unit volume per unit time) in a given four-dimensional region of space-time as a parameter of the spatial evolution of the interacting system. Such a quantitative estimate allows us to define the reaction zone, whose study offers the possibility of establishing the space-time structure of a fireball from the viewpoint of the interaction intensity at every point of space-time (for a study of the fireball structure in the momentum space using the number of reactions, see Refs. [9, 10]). At the same time, the regions of a fireball can be

distinguished by the total number of collisions which occur there. We use this quantity to determine the boundaries between different zones of reactions.

**Zones of reactions.** The number of reactions in the given space-time region can be determined with the use of the distribution function  $f(x, p)$ . For example, in the approximation of two-particle reactions  $2 \rightarrow 2$ , this function satisfies the Boltzmann equation [11]

$$p_1^\mu \partial_\mu f_1 = \int_2 \int_3 \int_4 W_{12 \rightarrow 34} (f_3 f_4 - f_1 f_2), \quad (1)$$

where the right-hand side contains the collision integral. The quantity  $W_{12 \rightarrow 34}$  is the transition rate which involves the reaction cross section and the conservation laws,  $\int_i \equiv \int \frac{d^3 p_i}{(2\pi)^3 E_i}$ ,  $f_i \equiv f(x, p_i)$  are one-particle distribution functions, and  $E_i = \sqrt{m_i^2 + \mathbf{p}_i^2}$  is the energy of a particle with momentum  $\mathbf{p}_i$ . The probability of a collision of two particles with momenta  $\mathbf{p}_1$  and  $\mathbf{p}_2$  corresponding to the distribution functions  $f_1$  and  $f_2$ , respectively, is determined at a space-time point  $x$  as  $\int_3 \int_4 W_{12 \rightarrow 34} f(x, p_1) f(x, p_2)$ . By integrating over the momenta of particles, we obtain the rate or the four-density of reactions at the point  $x$ :

$$\Gamma(x) = \int_1 \int_2 \int_3 \int_4 W_{12 \rightarrow 34} f(x, p_1) f(x, p_2). \quad (2)$$

Then, the number of reactions in the given space-time region  $\Omega$  is

$$N_{\text{coll}}(\Omega) = \int_\Omega d^4 x \Gamma(x). \quad (3)$$

It is seen that the number of reactions in the given space-time region depends on the four-density of reactions  $\Gamma(x)$ , which can be determined in a certain model approximation, e.g., like that in Refs. [12–14]. In particular,  $\Gamma(x)$  can be determined with the use of transport models.

Let us consider a large space-time region containing 99.99 % of all two-particle reactions and decays of resonances related to the event (a particular nucleus-nucleus collision). That is, the separated space-time region is so large that the dominant part of all reactions of hadrons

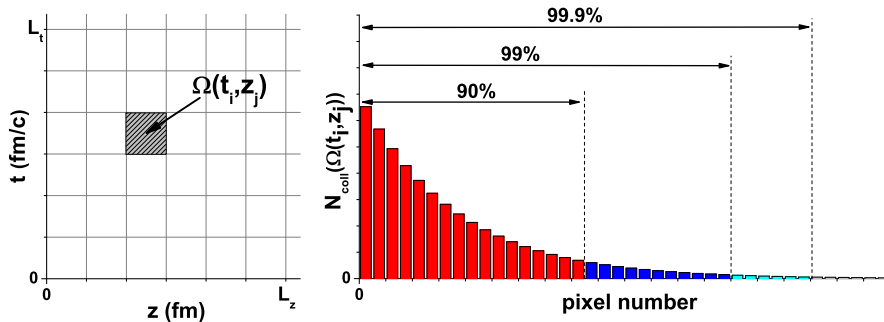


FIG. 1: (Color online) Algorithm of selection of pixels for the determination of the zone of reactions.

occurs in it. It can be a four-cube of reactions  $C_R$  with edges  $L_i$ , where  $i = t, x, y, z$ . To determine the zone of reactions, we divide the cube into separate equal parts (pixels), i.e., elements of the four-space, see Fig. 1 (left panel). Let  $\Omega = \Omega(t, \mathbf{r})$  be the four-volume of a pixel with coordinates of the center of this volume  $(t, \mathbf{r})$ . Totally, we have  $N_{\text{pix}} = L_t L_x L_y L_z / \Omega$  pixels. Then, for each four numbers  $(t, \mathbf{r})$ , we can calculate the absolute number of reactions in the given pixel  $\Omega(t, \mathbf{r})$  by using, e.g., formula (3). After this, we sort the pixels from left to right by the following hierarchy: from a pair of pixels, the left pixel is that in which a larger number of reactions has occurred. The arrangement of pixels is shown in Fig. 1 (right panel). The total area of the whole histogram (area covered by all bins) is equal to the total number of all hadron reactions  $N_{\text{tot}}$  in the four-cube of reactions  $C_R$ .

It is obvious that the problem of the determination of a space-time region, where all collisions have occurred, has a statistical character. Therefore, it is reasonable to search for this region with a certain precision. A small part of unaccounted reactions, to which we can refer also the decays of long-lived resonances, happens on such time intervals and at such distances which exceed the sizes of the four-cube of reactions  $C_R$ .

Let us sum the areas of bins beginning from the left according to the obtained hierarchy. We recall that the area of each bin gives the number of reactions in the corresponding pixel. In such a way, we can reach the value of the sum which is equal to a given number ( $\alpha_1 N_{\text{tot}}$ ), where  $\alpha_1$  is a part of the absolute number of all reactions  $N_{\text{tot}}$  (see Fig. 1). The hyperspace region which is occupied by the pixels contributing to this sum gives the reaction zone with the most intense reaction rate, and an  $\alpha_1$  piece of all hadronic reactions can be attributed to this four-volume.

Exploiting this algorithm, we follow to sum the area of bins to obtain a next ( $\alpha_2 N_{\text{tot}}$ ) number of reactions. These bins determine a neighboring four-volume region, where an  $\alpha_2$  piece of all hadronic reactions has occurred. Next, we determine a four-region which contains an  $\alpha_3$  piece of all reactions, and so on. Then,  $\alpha_1 + \alpha_2 + \alpha_3 + \dots = 1$ .

In the framework of this approach (algorithm), one can analyze a space-time structure of the fireball for different

species of particles and for different types of reactions, e.g., for elastic or inelastic reactions, decays, and so on. Obviously, this information gives insight into the dynamics and the structure of a particular nucleus-nucleus collision.

**Results of calculations.** To carry out calculations, we use the transport model UrQMD v2.3 [15, 16] which allows one to calculate the four-density of reactions at every point of the space-time region and to select reactions of a given type and for the given species of particles. In the present paper, we investigate, first, all possible hadron reactions and, second, just inelastic hadron reactions.

We take the number of reactions  $N_{\text{coll}}[\Omega(t, \mathbf{r})]$  in a pixel  $\Omega(t, \mathbf{r})$  as a result of the averaging over 1000 events. In the calculations, we took a four-cube of reactions  $C_R$  with the size of edges  $L_i = 200$  fm, where  $i = t, x, y, z$ .

In Figs. 2 and 3, we show the results of calculations for conditions at the BNL Alternating Gradient Synchrotron (AGS), Au+Au at 10.8A GeV, and at the CERN Super Proton Synchrotron (SPS), Pb+Pb at 158A GeV, in the case of central collisions. In accordance with the proposed algorithm, we determine the four-volume which contains 99% of all hadronic inelastic reactions,  $2 \rightarrow 2' + m, m \geq 0$  [depicted as the medium-gray (red) area]. We name this zone as a region of *hot fireball*. We determine also a four-volume that contains 99% of all possible hadronic reactions which include, of course, the previous zone. We name the region of 99% of all hadronic reactions excluding the zone of the hot fireball as a *cold fireball* [dark-gray (blue) area]. In fact, one can prefer another precision for the determination of zones of reactions.

By continuing to move along the hierarchical structure of pixels from left to right and by gathering a sum of the areas of their bins, i.e., the numbers of hadronic reactions corresponding to pixels, we determine those pixels which give, in total, for example, 0.9% of the total number of all reactions  $N_{\text{tot}}$ . This additional region can be named as a *fireball halo* [light-gray (cyan) area]. That is, the three space-time regions (hot, cold, halo) cover 99.9% of the total number  $N_{\text{tot}}$  of all hadronic reactions.

In Figs. 2 and 3, the rate of reactions is represented in the coordinates  $z$ - $t$ . That is, we deal with the cor-

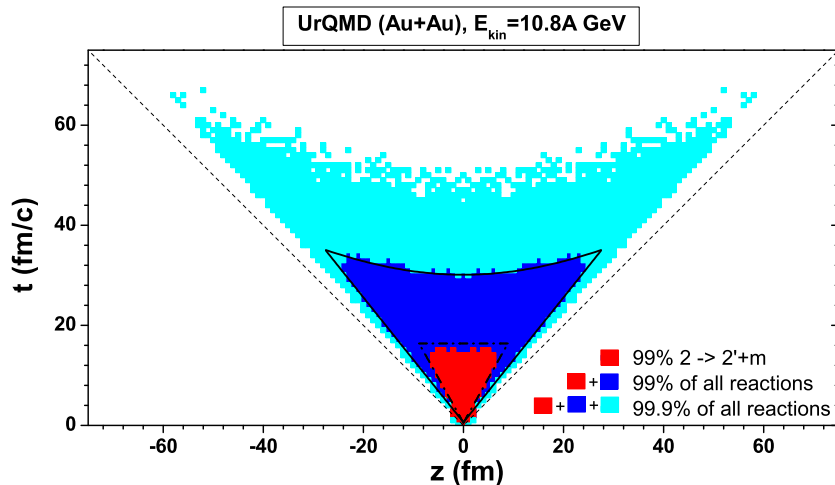


FIG. 2: (Color online) Projection of the reaction zone on the  $z$ - $t$  plane under the AGS (Au+Au at 10.8A GeV) conditions. The medium-gray (red) region contains 99% of all inelastic reactions,  $2 \rightarrow 2' + m, m \geq 0$ . The medium-gray (red) and the dark-gray (blue) regions together contain 99% of all hadronic reactions. The light-gray (cyan) region contains 0.9% of all hadron reactions only. The solid line bounds the region containing 99% of all reactions. The dashed-dotted line bounds the region containing 90% of all reactions.

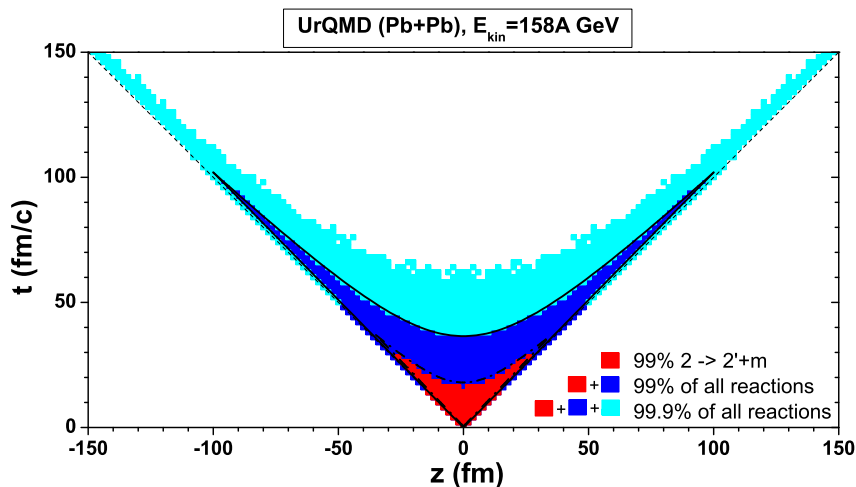


FIG. 3: (Color online) Same as Fig. 2, but for calculations under SPS conditions (Pb+Pb at 158A GeV).

responding projection of the four-volume of the zone of reactions on the  $z$ - $t$  plane. To construct this projection of the three-dimensional spatial pattern onto the  $z$  axis, we sum first all collisions along the transverse direction at the fixed coordinates  $(t, z)$ , namely [see Eq. (3)],

$$\tilde{N}_{\text{coll}}[\tilde{\Omega}(t, z)] = \int dx dy N_{\text{coll}}[\Omega(t, x, y, z)]. \quad (4)$$

Thus, we put a number of reactions  $\tilde{N}_{\text{coll}}$  in correspondence with the pixel  $\tilde{\Omega}(t, z)$  with the coordinates  $(t, z)$ . Then we construct the hierarchy of pixels  $\tilde{\Omega}(t, z)$  according to the above-mentioned sorting algorithm (see Fig. 1). It is seen that the interacting system has a comparatively long lifetime: A hot fireball decays completely only in the time intervals of the order of 15 fm/c for AGS and 35 fm/c for SPS. A cold fireball lives for 30–33 fm/c for AGS and 90–100 fm/c for SPS. Black solid lines show the approximation of the boundaries of the reaction zones.

By definition, the zones of hot and cold fireballs together contain 99% of all reactions. Moreover, the greater part of reactions outside of these zones consists of decays of resonances. If we follow the “classical” definition of

the sharp kinetic freeze-out hypersurface as some boundary that separates the interacting system from the space domain where particles do not interact, then we can regard the hypersurface which bounds the region of a cold fireball [the boundary between the dark-gray (blue) and light-gray (cyan) regions] as the sharp freeze-out hypersurface.

For both collision energies of nuclei under consideration, the upper parts of freeze-out hypersurfaces in Figs. 2 and 3 are the space-like hyperbolas, which have the form of constant proper-time surfaces to within some factor, namely,  $t(z) = A\sqrt{\tau_0^2 + z^2}$ , where  $A = 0.65$ ,  $\tau_0 = 46$  fm/c for AGS energies and  $A = 0.95$ ,  $\tau_0 = 38$  fm/c for SPS energies. From the bottom a cold fireball is bounded by the time-like hypersurface, which has the form of a straight line  $t(z) = t_0 + \frac{1}{v}z$ , where  $t_0$  is approximately zero, and  $v = 0.8$  for AGS energies and  $v = 0.98$  for SPS energies.

The results of evaluations of the time dependence of the reaction rates integrated over the total spatial volume (frequency of reactions) are depicted in Figs. 4 and 5. The thick solid line indicates all reaction rates in the

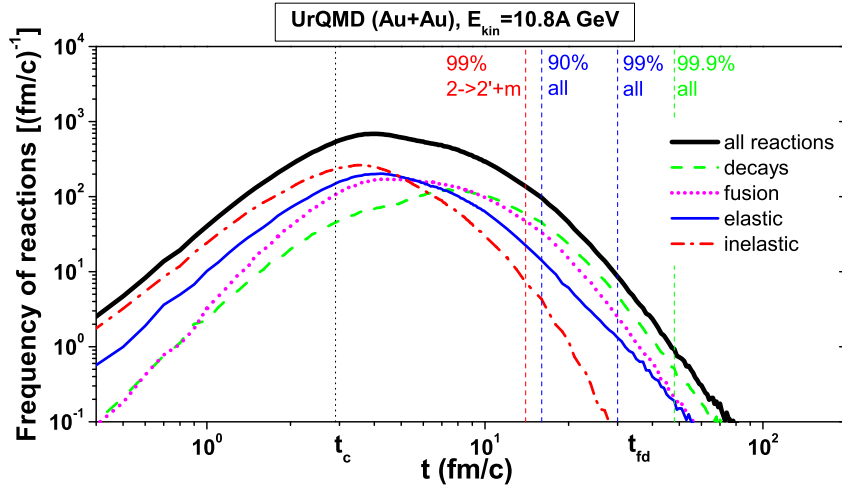


FIG. 4: (Color online) Frequency of the hadron reactions (reaction rates integrated over the total spatial volume) for AGS conditions (Au+Au at 10.8A GeV). Different curves correspond to different types of reactions. Vertical lines indicate the time moments of the margins of zones of reactions for the point  $z = 0$  (see Fig. 2).

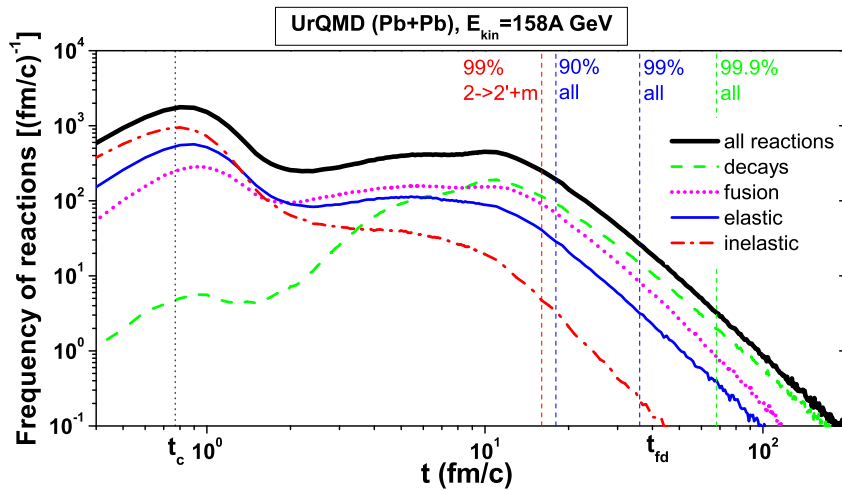


FIG. 5: (Color online) Same as Fig. 4, but for the SPS conditions (Pb+Pb at 158A GeV).

fireball, the thin solid line indicates just the elastic scattering of hadrons ( $2 \rightarrow 2$ ), the dash-dotted line shows all inelastic reactions ( $2 \rightarrow 2' + m$ , where  $m \geq 0$ ), the dotted line stands for fusion reactions ( $2 \rightarrow 1'$ ), and the dashed line distinguishes decays ( $1 \rightarrow 2' + m$ ,  $m \geq 0$ ). Note that the compound-elastic reactions (pseudoelastic in Ref. [17]) such as  $2 \rightarrow \rho \rightarrow 2$  are separated in two parts; the first part  $2 \rightarrow \rho$  is incorporated to the reactions of fusion, and the second part  $\rho \rightarrow 2$  to the reactions of decay.

The main feature of the frequency of all reactions (thick solid lines in Figs. 4 and 5) is its increase up to  $t \approx 3.9$  fm/c for AGS energies and  $t \approx 0.84$  fm/c for SPS energies. This can be explained by increasing the number of nucleons as participants of the reactions, when one nucleus penetrates into another one. Indeed, the maximum overlap of two nuclei happens if their centers coincide. This time can be estimated as

$$t_c = \frac{R_0}{\gamma} \frac{1}{v}, \quad (5)$$

where  $R_0$  is the nucleus radius,  $v = p_{0z}/\sqrt{M_N^2 + p_{0z}^2}$ ,  $\gamma = 1/\sqrt{1-v^2}$ ,  $p_{0z}$  is the initial nucleon momentum in the

c.m. system of two nuclei, and  $M_N$  is the nucleon mass. In what follows, we name  $t_c$  as the *fireball formation time*. For two experiments under consideration, this gives  $t_c = 2.9$  fm/c for AGS (10.8A GeV) and  $t_c = 0.77$  fm/c for SPS (158A GeV). These values are very close to the time moments which correspond to the first maximum of the frequency of all reactions (thick solid lines in Figs. 4 and 5) and local maxima of the particular types of reactions for SPS conditions, see Fig. 5. Slight difference of  $t_c$  and the time point of the real maximum can be explained by some decrease of a nucleon velocity which is due to inelastic and elastic reactions (stopping) of nucleons. The same behavior can be seen as well in Ref. [17], Fig. 1, obtained from UrQMD calculations for SPS conditions (Pb-Pb,  $E_{\text{kin}} = 158A$  GeV).

Inelastic nucleon collisions dominate at the first stage,  $t \lesssim t_c$ , of nucleus-nucleus collision. At later times, the elastic and fusion reactions become more significant. We note that for both energy conditions, the decay processes become the dominant ones after  $t \approx 10$  fm/c.

After the full overlap of the nuclei, the created system begins to expand in space, which results in a decrease of the reaction rates. At the same time, the number of sec-

ondary particles still increases, resulting in an increase of the total reaction integral rate. Hence, the rate of expansion of the system and its ratio to the creation rate of secondary particles will determine the result of the competition of these two tendencies. A similar competition was investigated in Ref. [14], where on this basis some conclusions about freeze-out were made.

The number of secondary particles (mainly  $\pi$  mesons) is approximately  $\langle n_\pi \rangle \approx 1.6$  per nucleon for AGS conditions and  $\langle n_\pi \rangle \approx 6$  for SPS conditions. Such an increase of the number of secondary particles with the collision energy leads to the sufficient difference of dependences of the frequency of reactions on time. Namely, for AGS conditions after  $t_c$ , the the frequency of all reactions goes down, which results in *fireball division* into two parts at the time moment  $t = t_{fd}$  and the further breakup. The *fireball division time* is defined as the minimum value of time on the space-like hypersurface, which bounds the region of the cold fireball (blue area) from above, i.e.,  $t_{fd} \equiv t(z)|_{z=0}$  (see Figs. 2 and 3). For SPS conditions, one can see the second local maximum of the frequency of reactions (see thick solid line in Fig. 3) at  $t_M \approx 10.6$  fm/c which is a consequence of a large number of reactions with secondary particles. This results in an increase of the *fireball lifetime*:

$$\tau = t_{fd} - t_c. \quad (6)$$

We note that the time moment  $t_{fd}$  depends very weakly on the collision energy.

It is seen that at  $z = 0$  in the c.m. system after the time moment  $t_{fd}$ , the rates of elastic and inelastic reactions vanish. That is, since this moment, the system behavior is determined mainly by the individual properties of particles (basically resonances). That is why, in spite of the sufficient difference of collision energies of the experiments under consideration, the times  $t_{fd}$  are approximately the same. If we compare the longitudinal sizes of the fireballs  $2R_z$  at the time moment  $t = t_{fd}$ , we see that they are approximately the same and equal to  $R_z = v t_{fd}$  [ $v$  is defined in Eq. (5), see Figs. 2 and 3]. This fact can explain the weak dependence of the pion interferometric radius  $R_L$  on the beam energy,  $R_L \propto R_z$  [18]. It can be claimed that the fireball achieves its maximum longitudinal size at the time moment  $t = t_{fd}$ , when it is divided into two parts.

**Discussion and Conclusions.** The main idea of the method proposed for analyzing the fireball structure is the determination of the hierarchy of hadronic reactions in accordance with their intensity (rate), see Fig.1. In view of the hierarchy obtained, we formulate an algorithm for the determination of the zones of reactions of the interacting system: we divide the fireball space-time volume into different regions. *By definition, we recognize a specific zone of reactions (elastic, inelastic, etc.) as a four-volume, where 99% of a given specific type of reactions have occurred.*

In the present microscopic study, we separate a fireball into the following regions, which characterize its

evolution (see Figs. 2 and 3): (1) a hot fireball region, where 99% of all inelastic hadronic reactions have occurred (medium-gray or red), (2) a cold fireball region (dark-gray or blue), which together with the hot fireball contains 99% of all hadronic reactions  $N_{tot}$ , and (3) a fireball halo, where 0.9% of all hadronic reactions, i.e.,  $0.009N_{tot}$ , have occurred (light-gray or cyan). Two last regions together are a space-time region containing the hadron-resonance gas, and the reactions in this region are mainly presented by decays of resonances.

An important question that can be clarified by the study of the zone of reactions is how the space-time boundary of a fireball is related to the so-called sharp freeze-out hypersurface. In the literature, the sharp freeze-out hypersurface is defined with the help of some parameter  $P(t, \mathbf{r})$  which takes the critical value  $P_c$  on the hypersurface. That is, the equation of the hypersurface has form  $P(t, \mathbf{r}) = P_c$ . As such a parameter, one may choose the energy density  $\epsilon(t, \mathbf{r})$  [4, 6], temperature  $T(t, \mathbf{r})$  [19, 20], density of particles  $n(t, \mathbf{r})$  [21], etc. *It is necessary to note that any definition of the sharp freeze-out is possible just with chosen accuracy.*

One can follow the ‘‘classical’’ definition: the sharp kinetic freeze-out hypersurface is an imaginary hypersurface, outside of which there are no collisions between particles of the system. In other words, the sharp kinetic freeze-out hypersurface is determined as a surface bounding the space-time region, in which almost all collisions between hadrons of the system happened (for example, 99%). Thus, we can identify the reaction zone boundary and the sharp kinetic freeze-out hypersurface. Then the boundary between the zone of a cold fireball and the fireball halo, can be interpreted as a sharp kinetic freeze-out hypersurface (see Figs. 2 and 3). In the coordinates  $(t, z)$ , the space-time part of this hypersurface is a hyperbola and has the form  $t(z) = A\sqrt{\tau_0^2 + z^2}$ , where  $A = 0.65$ ,  $\tau_0 = 46$  fm/c for the AGS energy ( $E_{kin} = 10.8A$  GeV) and  $A = 0.95$ ,  $\tau_0 = 38$  fm/c for the SPS energy ( $E_{kin} = 158A$  GeV). It is clear that the *fireball division time* is related to the parameters of the hyperbola in the following way  $t_{fd} = A\tau_0$  and we obtain  $t_{fd} \approx 30$  fm/c for AGS ( $E_{kin} = 10.8A$  GeV) and  $t_{fd} \approx 36$  fm/c for SPS ( $E_{kin} = 158A$  GeV).

The lower time-like hypersurface bounding a cold fireball has the form of a straight line  $t(z) = t_0 + \frac{1}{v}z$ , where  $t_0$  is close to zero, and  $v = 0.8$  for AGS energies and  $v = 0.98$  for SPS energies. For AGS energies,  $E_{kin} = 10.8A$  GeV, the time-like boundaries of the reaction zones differ significantly from one another and the light cone (see Fig. 2). However, at higher SPS energies, for example, at  $E_{kin} = 158A$  GeV, the time-like hypersurfaces bounding all three zones of a fireball practically coincide with one another and are close to the light cone (see Fig. 3). Thus, we can predict that this behavior will result in all time-like hypersurfaces merging on the energies available at the BNL Relativistic Heavy Ion Collider (RHIC) and coinciding with the light cone.

On the base of the same ideology, we can define the

sharp chemical freeze-out hypersurface. Namely, the hypersurface separating the zones of the hot and cold fireballs can be associated with the sharp chemical freeze-out with an accuracy of 99% (we assume that the chemical freeze-out occurs when the inelastic reactions are completed [22]).

On the other hand, if one deals with a continuous freeze-out, for instance, by fixing the coordinates of the last collisions, then the set of these points (with an accuracy of 99%) will be inside the boundaries we determined above.

On the basis of the analysis of the time dependence of

the frequency of reactions (see Figs. 4 and 5), we conclude that there are two specific time points in the evolution of a hadron fireball: the *fireball formation time*  $t_c$  defined as the time of the full overlap of two nuclei [Eq. (5)] and the *fireball division time*  $t_{fd}$  which corresponds to the separation of the fireball into two individual parts.

**Acknowledgments.** The authors thank L. McLerran, P. Romatschke, and V. Magas for useful discussions. The authors also greatly appreciate the valuable comments made by the referee.

- 
- [1] R. Baier, A.H. Mueller, *et al.*, Phys. Lett. B **502**, 51 (2001); arXiv:hep-ph/0009237.
  - [2] P. Arnold, J. Lenaghan, G.D.Moore, and L.G.Yaffe, Phys. Rev. Lett. **94**, 072302 (2005); arXiv:nucl-th/0409068.
  - [3] A. Rebhan, P. Romatschke, and M. Strickland, Phys. Rev. Lett. **94**, 102303 (2005); arXiv:hep-ph/0412016.
  - [4] V.N. Russkikh and Y.B. Ivanov, Phys. Rev. C **76**, 054907 (2007); arXiv:nucl-th/0611094.
  - [5] T. Csorgo, *et al.*, Phys. Lett. B **565**, 107 (2003); arXiv:nucl-th/0305059.
  - [6] J. Sollfrank, P. Huovinen, and P.V. Ruuskanen, Eur. Phys. J. C **6**, 525 (1999); arXiv:nucl-th/9801023.
  - [7] D. Molnar and M. Gyulassy, Phys. Rev. C **62**, 054907, 2000; arXiv:nucl-th/0005051.
  - [8] A. Kisiel, W. Florkowski, W. Broniowski, and J. Pluta, Phys. Rev. C **73**, 064902 (2006); arXiv:nucl-th/0602039.
  - [9] D. Anchishkin, A. Muskeyev, and S. Yezhov, Nucl. Phys. A **820**, 307C (2009); arXiv:0902.0999 [nucl-th].
  - [10] D. Anchishkin, A. Muskeyev, and S. Yezhov, Int. J. Mod. Phys. A **24**, 4437 (2009); arXiv:0902.4171 [nucl-th].
  - [11] S.R. de Groot, W.A. van Leeuwen, and Ch.G. van Weert, *Relativistic Kinetic Theory*, (North-Holland, Amsterdam, 1980).
  - [12] K.J. Eskola, H. Niemi, P.V. Ruuskanen, Phys. Rev. C **77**, 044907 (2008); arXiv:0710.4476.
  - [13] B. Tomasik and U.A. Wiedemann, Phys. Rev. C **68**, 034905 (2003); arXiv:nucl-th/0207074.
  - [14] C.M. Hung and E. Shuryak, Phys. Rev. C **57**, 1891 (1998); arXiv:nucl-ph/9709264.
  - [15] S.A. Bass *et al.*, Prog. Part. Nucl. Phys. **41**, 225 (1998); arXiv:nucl-th/9803035.
  - [16] M. Bleicher *et al.*, J. Phys. G **25**, 1859 (1999).
  - [17] M. Bleicher and J. Aichelin, Phys. Lett. B **530**, 81 (2002); arXiv:hep-ph/0201123.
  - [18] J. Chen (for STAR Collaboration), in CPOD2009 *Proceedings*, PoS (CPOD2009)047 (SISSA, Trieste, Italy, 2009); arXiv:0910.0556 [nucl-ex].
  - [19] H. von Gersdorff, L. McLerran, M. Kataja, and P.V. Ruuskanen, Phys. Rev. D **34**, 794 (1986).
  - [20] P. Huovinen, Eur. Phys. J. A **37**, 121 (2008); arXiv:0710.4379.
  - [21] D.Adamova *et al.* (CERES Collaboration), Phys. Rev. Lett. **90**, 022301 (2003); arXiv:nucl-ex/0207008.
  - [22] U. Heinz, Nucl. Phys. A **661**, 349 (1999); Nucl. Phys. A **685**, 414 (2001).